Hindawi Publishing Corporation
International Journal of Antennas and Propagation
Volume 2015, Article ID 715958, 8 pages
http://dx.doi.org/10.1155/2015/715958

Research Article

A CPW-Fed Quasi-PIFA Antenna Using Quasi-Lumped Resonators for Mobile Phones

Majid Rafiee, Mohd Fadzil bin Ain, and Aftanasar Md. Shahar

School of Electrical and Electronics Engineering, Universiti Sains Malaysia, Engineering Campus Seberang Perai Selatan, 14300 Nibong Tebal, Penang, Malaysia

Correspondence should be addressed to Majid Rafiee; rafiee6@gmail.com

Received 27 July 2014; Revised 2 November 2014; Accepted 3 November 2014

Academic Editor: Sai-Wai Wong

A novel single CPW-fed Quasi-Planar Inverted-F Antenna (PIFA) using quasi-lumped elements is developed for mobile communication handheld terminals operating at 2.6 GHz. The antenna is composed of an inductor covered by a set of interdigital and parasitic capacitors. The proposed antenna achieves a measured bandwidth of 11% for return loss with the antenna gain of about 4 dBi. The antenna is designed in single layer (zero height) which is appropriate to be used in thin devices where a small room is considered for the antenna. The proposed antenna is suitable for use in Long Term Evolution band 7. The operating frequency of introduced antenna depends on the number of interdigital fingers and inductor length rather than the total resonator patch only, so that the operating frequency can be altered while the total patch size remains unchanged. The calculated operating frequency is confirmed by simulation and measurement. Also the dipole-like simulated radiation pattern is confirmed by measurement.

1. Introduction

Nowadays, wireless devices have a vital role of having almost constant connectivity worldwide. By decreasing the size of future wireless devices, there is a corresponding demand for similar size reduction in antenna elements, as well. However the performance of the antenna strongly depends on its size so that it becomes more complicated in contrast to the complexity which communication infrastructure is faced with [1]. The present-day challenge for antenna designers is to provide wide bandwidth, high efficiency while reducing the equipment size. Planar Inverted-F Antenna (PIFA) which resonates at quarter-wavelength is an ideal choice for mobile phones for its low profile and low inherent signal absorption ratio (SAR) compared to the patch antennas.

Numerous researches have been done on widening and CPW-fed techniques of not only monopole antennas [2, 3] but also PIFA antennas in terms of bandwidth enhancement [4], single/multiple resonant frequencies [5, 6], reconfigurability [7], tunability [8], and radiation pattern improvement [9]. PIFA is better choice for cellphones antennas where a limited space is considered for the antenna to be integrated. The conventional internal PIFA antennas have a high profile of almost up to 10 mm on the top of ground plane in order to get wide bandwidth. However the PIFA's bandwidth strongly depends on the vertical distance between the resonating strip and ground plane while in the recent cell phones, thin profile is more attracted in the market. Although PIFA occupies much smaller space, its 3-dimensional structure where the patch is located above the system ground plane leads to occupying high profile and being more structurally challenging as compared to 2-dimensional planar antennas.

Like other kind of antennas, miniaturizing is an interesting challenge which many of researchers face. Many techniques are introduced to miniaturize the size of this kind of antenna such as using meander line or capacitive loading. A reconfigurable multiband planar antenna is presented in [10] which has 2D structure where a MEMS switch operates as a short-circuited in ON state which enables the antenna to resonate at quarter-wavelength. A planar printed PIFA antenna using a resonating strip is also introduced in [11]. In this paper an alternative single-feed structure of PIFA antenna using quasi-lumped elements in only a single layer is presented where it can satisfy the desired characteristics of

PIFA antennas while not only does it have 2D structure, but also the bandwidth is not sensitive to the antenna height.

The *LC* resonators are commonly used in dipole and multifrequency monopole antennas. However, [12] introduced a new approach in PIFA design by employing the *LC* resonator as a resonating strip. A network of interdigital and parasitic capacitors and an inductor to shape the main resonating element are presented in this paper. However the interdigital capacitors are widely used in filters. It is also used as a feeding structure for impedance matching in [13]. However, it has not, to our knowledge, been used neither as a main resonator in antenna nor in PIFA designs. It will be shown that by using this shape, the operating frequency does not depend on wavelength directly since it can be tuned by adjusting the numbers of interdigital capacitors, inductor length, and capacitors width while the total size of the patch is unchanged. Next section presents the antenna's structure which can be located on the back cover of cellphones.

2. Antenna Design

2.1. Inductor's Inductance and Interdigital Capacitors' Capacitance. A deep analysis on both radiating and balanced mode of PIFA antenna and its impedance variation is done by [14]. The 10 × 8 mm resonator element contains *quasi-lumped elements* including an inductor covered by a set of interdigital capacitors and two parasitic capacitors on the same layer where the ground plane is located. The inductor L with the length of L_I is covered by two sets of multifinger interdigital capacitors with the length of L_c at the center of the resonator which are shown in Figure 1. The inductance can be increased by increasing the length of inductor line L_I (i.e., using the meander line). On the other hand, the number of fingers can control the capacitance of the interdigital capacitors. The inductance of the inductor and capacitance of the interdigital capacitors per unit length along H_q can be calculated using (1) [15] and (2) [16], respectively, as follows:

$$L = 200 \times 10^{-9} L_I \left[\ln\left(\frac{2L_I}{W_I + t} \right) + \left(0.50049 + \frac{W_I}{3L_I} \right) \right], \tag{1}$$

$$C_I = \left(\epsilon_r + 1\right) L_C \left[(N-3) A_1 + A_2 \right] \ \left(\text{pF/unit length}\right), \tag{2}$$

where t is metal thickness, ϵ_r is the substrate permittivity, N is number of fingers, and A_1 and A_2 are the capacitance per unit length of the fingers and can be calculated by

$$A_1 = 4.409 \tanh\left[0.55 \left(\frac{h}{W_C} \right)^{0.45} \right] \times 10^{-6} \ \left(\text{pF}/\mu\text{m}\right),$$
$$A_2 = 9.920 \tanh\left[0.52 \left(\frac{h}{W_C} \right)^{0.50} \right] \times 10^{-6} \ \left(\text{pF}/\mu\text{m}\right). \tag{3}$$

The general expression for total series capacitance of an interdigital capacitor can also be expressed by [17]

$$C_I = 2\epsilon_0 \epsilon_{re} \frac{K(k)}{K(k')} (N-1) L_C \ \text{(F)} = \frac{10^{-11}}{18\pi} \epsilon_{re} \frac{K(k)}{K(k')} (N-1) L_C \times 10^{-4} \ \text{(F)}, \tag{4}$$

$$C_I = \frac{\epsilon_{re} 10^{-3}}{18\pi} \frac{K(k)}{K(k')} (N-1) L_C \ \left(\text{pF}\right), \tag{5}$$

where L_C is in microns and ϵ_{re} is the effective dielectric constant of the micrstrip line of width of W and can be achieved by

$$\epsilon_{re} = \frac{(\epsilon_r + 1)}{2} + \frac{(\epsilon_r - 1)}{2} \left[1 + \frac{10h}{W} \right]^{-0.5}. \tag{6}$$

Also the ratio of complete elliptic integral of first kind $K(k)$ and its complement $K(k')$ is given by

$$\frac{K(k)}{K(k')} = \frac{1}{\pi} \ln\left[2 \left(\frac{1 + \sqrt{k}}{1 - \sqrt{k}} \right) \right] \quad \text{for } 0.707 \le k \le 1, \tag{7a}$$

$$\frac{K(k)}{K(k')} = \frac{\pi}{\ln\left[2 \left(\left(1 + \sqrt{k'}\right) / \left(1 - \sqrt{k'}\right) \right) \right]} \quad \text{for } 0 \le k \le 0.707, \tag{7b}$$

where

$$k = \tan^2\left(\left(\frac{\pi}{4} \right) \left(\frac{W_C}{W_C + D_G} \right) \right); \quad k' = \sqrt{1 - k^2}. \tag{8}$$

In this paper, $W_C = D_G$, the ratio of elliptic integral is unity, so that (5) can be simplified to

$$C_I = \epsilon_0 \left(\frac{\epsilon_r + 1}{2} \right) \left[(N - \Delta) L_C \right], \tag{9}$$

where Δ is the value of width correction factor (the edge effect of the first and last fingers) and can be approximated to 0.44, 0.65, and 0.5 for $N = 1$, $N = 2$, and $N \ge 3$, respectively [16, 18].

2.2. Parasitic Capacitor's Capacitance. Figure 1 depicts two capacitors known as parasitic capacitors, C_{P_1} and C_{P_2}, respectively. The value of C_{P_1} and C_{P_2} can be determined using the three-dimensional finite difference method which was proposed by [19]. The capacitance of coplanar parasitic capacitors can be calculated using

$$C_{P_i} = \frac{\left(Q_{\text{total}} - X \cdot Q' \right)}{V}; \quad i = 1, 2, \tag{10}$$

where Q_{total} is the total charge on the conductor, Q' is the charge per unit length on the connected microstrip transmission line, V is the potential difference between patch conductor and ground plane, and X is the distance between the back-transformed reference plane of discontinuity and the magnetic wall (transmission lines are considered to be surrounded by a shield of magnetic and electric walls). Q_{total} and Q' are needed to calculate C_{P_i} in (10).

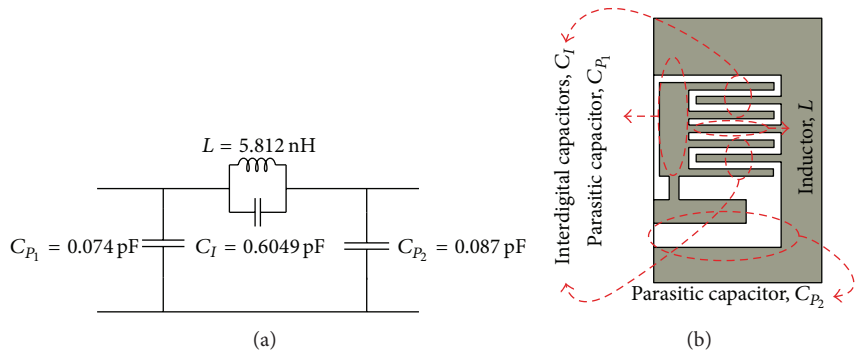

Figure 1: (a) Equivalent circuit and (b) inductor and parasitic/interdigital capacitors scheme.

2.2.1. Q'. The charge per unit on the connected transmission line can be obtained by

$$Q' = \epsilon_0 \epsilon_r \oint_C E_n \cdot ds, \tag{11}$$

where C is the delineation of integration section which surrounds the cross section at the plane of the magnetic wall and E_n is the electrical filed distribution on n times repeated grid sections. The accuracy of these potentials appertain on the number of n so that having more iteration parts increases the accuracy. According to [19], $n = 60$ is good enough to an accuracy better than 1% for calculating equivalent capacitance of an open-ended microstrip line. By applying the boundary conditions to Taylor's series expansion, the electrical potential Φ in the immediate vicinity inside the $x - z \geq 0$ plane of each point can be calculated by

$$\begin{aligned}\Phi = &\left(\frac{d\epsilon_1 + c\epsilon_2}{ab} + \frac{\epsilon_1}{d} + \frac{\epsilon_2}{C} + \frac{d\epsilon_1 + c\epsilon_2}{ef}\right)^{-1} \\ &\times \left(\frac{d\epsilon_1 + c\epsilon_2}{a(a+b)}\Phi_A + \frac{d\epsilon_1 + c\epsilon_2}{b(a+b)}\Phi_B + \frac{\epsilon_2}{c}\Phi_C\right. \\ &\left. + \frac{\epsilon_1}{d}\Phi_D + \frac{d\epsilon_1 + c\epsilon_2}{e(e+f)}\Phi_E + \frac{d\epsilon_1 + c\epsilon_2}{f(e+f)}\Phi_F\right),\end{aligned} \tag{12}$$

where a, b, c, d, e, and f are the distance of calculated potential points from the considered point which are shown in Figure 2. For instance (13) and (14) deliver the optimum value of electrical potential for two desired points at position P and Q, respectively, as follows:

$$\begin{aligned}\Phi_P = &\left(\frac{1}{a+b}\right)(bcdef\Phi_A + acdef\Phi_B) \\ &+ \left(\frac{1}{c+d}\right)(abdef\Phi_C + abcef\Phi_D) \\ &+ \left(\frac{1}{e+f}\right)(abcde\Phi_E + abcde\Phi_F),\end{aligned} \tag{13}$$

$$\begin{aligned}\Phi_Q = &\left(\frac{e+f}{2}\right)(bcdef\Phi_A + acdef\Phi_B) \\ &+ \left(\frac{\epsilon_r(a+b)(e+f)}{2(\epsilon_r d + c)}\right)\left(\frac{abdef}{\epsilon_r}\Phi_C + abcef\Phi_D\right) \\ &+ \left(\frac{a+b}{2}\right)(abcdf\Phi_E + abcde\Phi_F) \\ &- (a+b)(c+d)(e+f).\end{aligned} \tag{14}$$

The electrical field at each grid section can be achieved by

$$\vec{E} = -\vec{\nabla}\Phi. \tag{15}$$

The electrical potential can be calculated using Laplace's equation as a linear combination of finite difference expression of neighboring grid points at each grid point inside the shield [19]. Using "relaxation method," (16) will be achieved as follows:

$$\Phi_{\text{new}} = \Phi_{\text{old}} - K \cdot R, \tag{16}$$

where K is the relaxation constant and assigns the speed of convergence. Naghed and Wolff [19] state the optimal value of 1.8 for this solution.

2.2.2. Q_{total}. The total charge on the conductor can be calculated using the electrical field distribution as follows:

$$Q_{\text{total}} = \epsilon_0 \epsilon_r \iint_A \vec{E} \cdot \vec{n}\, dx\, dz. \tag{17}$$

Let us assume that the distances to the back and lateral electric walls ($X/2$ and $Z/2$) and also to the magnetic wall and to the upper surface ($Y/2$) are all equal to h. The potentials are presumed to be $\Phi_1 = \Phi_2 = 1$ V and zero on the ground plane ($\Phi_0 = 0$). Hence the equivalent capacitances C_{P_1} and C_{P_2} can be achieved as follows:

$$\begin{aligned}C_{P_1} &= \left(Q_{1_{\text{total}}} - X_1 \cdot Q_1'\right), \\ C_{P_2} &= \left(Q_{2_{\text{total}}} - X_2 \cdot Q_2'\right).\end{aligned} \tag{18}$$

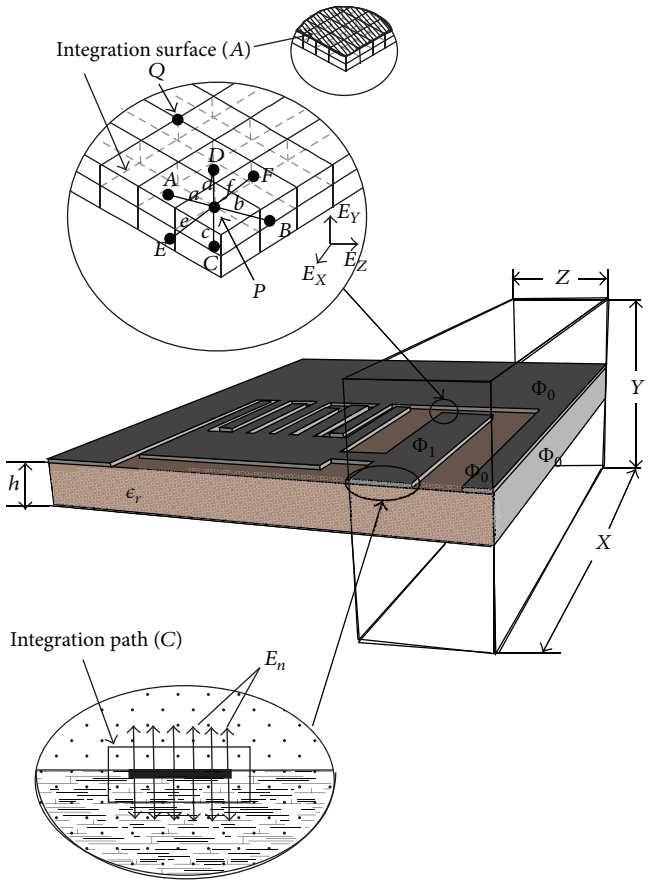

Figure 2: Calculation of total charge and charge per unit length for the first parasitic capacitor.

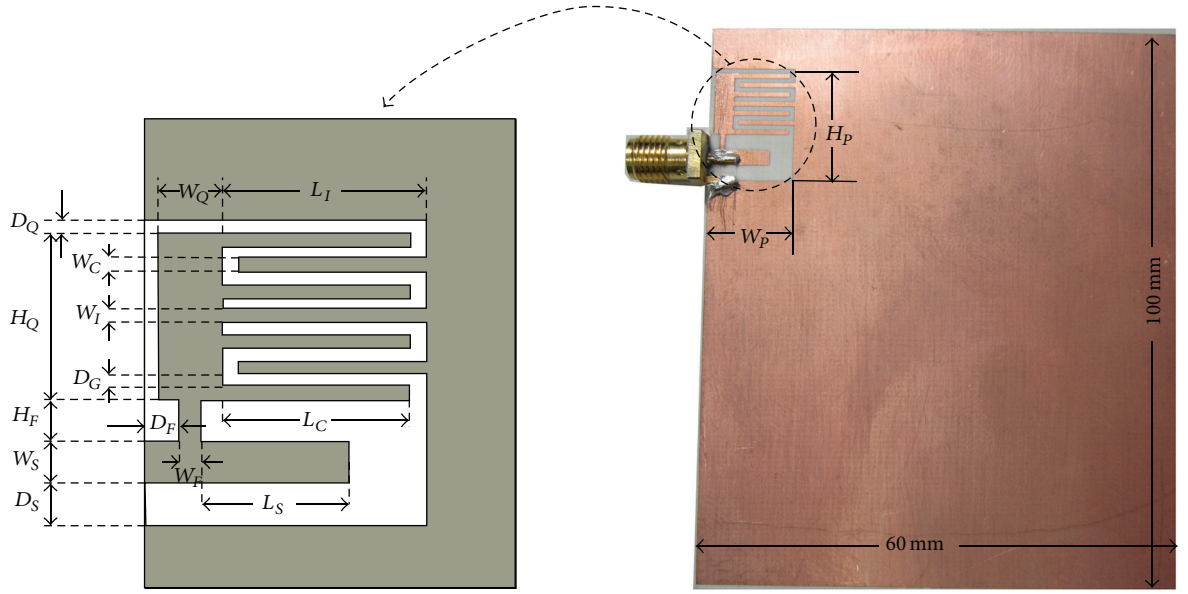

Figure 3: The geometry of the printed CPW-feeding structure of PIFA using quasi-lumped *LC* resonators.

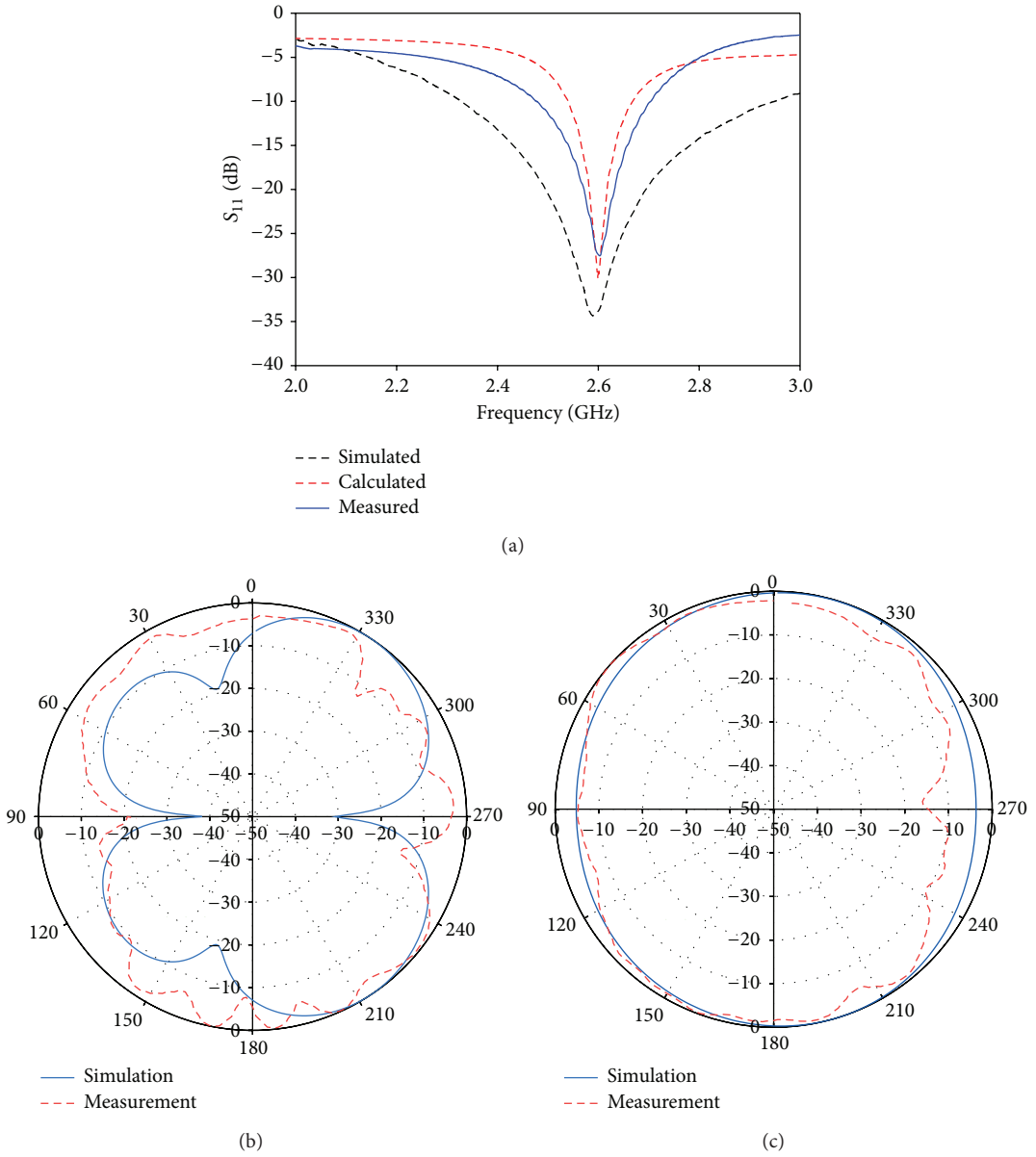

FIGURE 4: (a) Simulated, calculated, and measured return loss and radiation pattern for (b) E-Plane and (c) H-Plane.

The calculated values (which are shown in Figure 1(a)) of $L, C_I, C_{P_1}(W/h \approx 2.45)$ and $C_{P_2}(W/h \approx 3.08)$ are 5.812 nH, 0.6049 pF, 0.074 pF, and 0.087 pF, respectively. Finally, the resonant frequency can be achieved by

$$f = \frac{1}{2\pi\sqrt{L\left(\left(C_{P_1}C_{P_2}/\left(C_{P_1}+C_{P_2}\right)\right)+C_I\right)}}. \quad (19)$$

3. Results

Figure 3 exhibits the printed antenna's prototype on a Duriod R4003c substrate with 100 × 60 × 0.813 mm dimensions and $\epsilon_r = 3.38$. The antenna has been measured and successfully verified at the Penang Skills Development Centre (PSDC). The simulated and measured results are shown in Figure 4. In accordance with the measured results for the 6 dB return loss specifications in Figure 4(a), it implies that the antenna operates at LTE band 7 with 83% of radiation efficiency. In addition, the simulated Smith chart and current distribution are illustrated in Figures 5(a) and 5(b), respectively.

Equation (19) can explain a distinct advantage of the proposed antenna which depends on the wavelength indirectly. This means that the resonant frequency can be tuned by number, width, and length of fingers while the total patch size remains unchanged. The term *indirectly* is used since still the resonance of antenna depends on the wavelength since by varying the overall dimensions of the patch either in H_Q or W_Q, the resonant frequency will be shifted. However, as it can be observed, the antenna specifications can be controlled by tuning the capacitance and inductance by adjusting the value of controlling parameters.

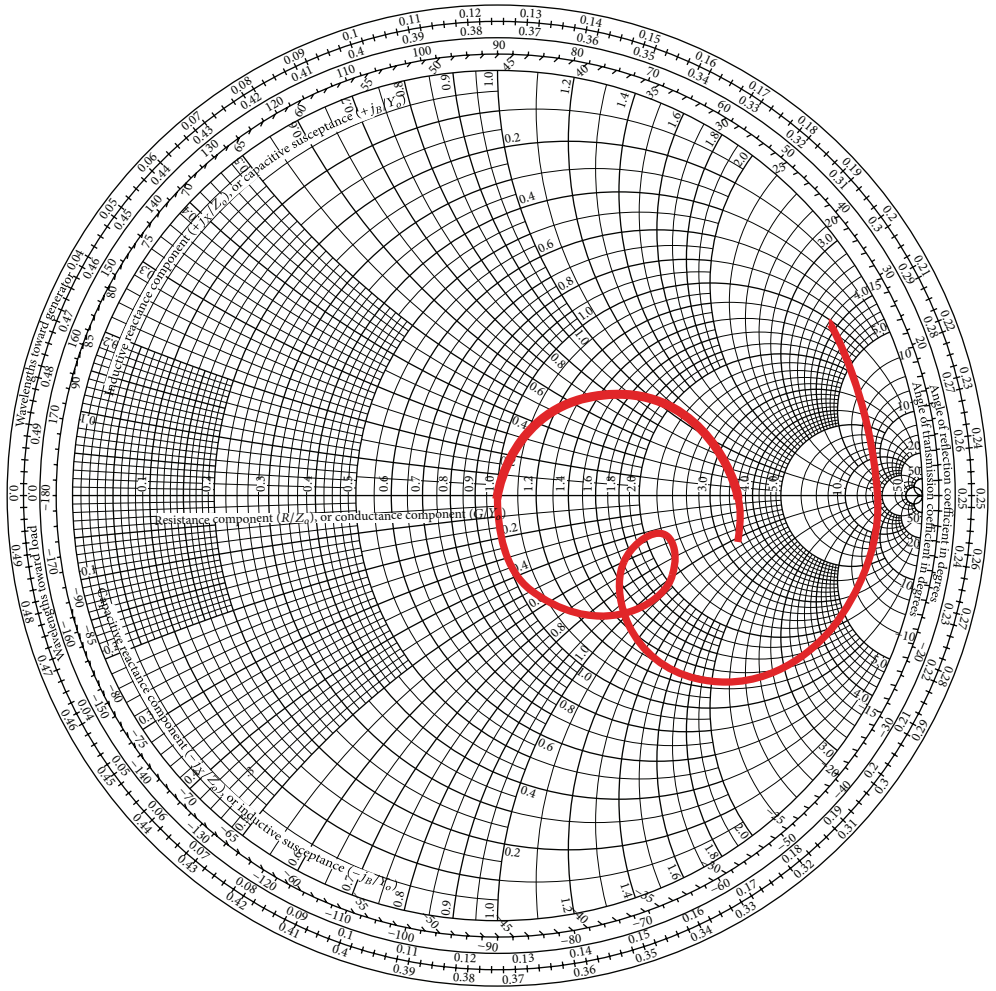

Figure 5: (a) Simulated Smith chart and (b) current distribution.

The first parasitic capacitor is controlled by L_S and W_S. The second parasitic capacitor also can be adjusted using W_Q and H_Q. The inductor length (L_I), interdigital capacitors width (W_C), and total number of interdigital capacitors fingers play a critical role in determining not only operating frequency, but also the bandwidth of this kind of antenna. The value of these parameters is quite sensitive since not only do they have direct effect on antenna operating frequency, but also the input impedance can be matched by using the right value for them. In present study, the W_S is arrogated to cover

Table 1: Parametres.

Parameter	Size (mm)	Parameter	Size (mm)
H_P	15	W_S	1.989
H_Q	8	L_I	7.835
H_F	2	L_C	7.22
W_P	10.835	L_S	5.735
W_Q	2.5	D_F	1.4
W_F	0.7	D_G	0.615
W_C	0.615	D_S	0.615
W_I	0.615	D_Q	2

LTE band 7. For sure, other geometry parameters affect the impedance matching, as well. All the optimized parameters are summarized in Table 1 to achieve the optimum value.

Furthermore the measured and simulated radiation patterns at center frequency are plotted in Figures 4(b) and 4(c). Dipole-like patterns are observed, which illustrate no outstanding difference compared to regular internal mobile antennas and are almost the same to those seen in them. The slight distinctions can be imputed to the feeding cable influences on the antenna radiation patterns.

4. Conclusion

A quasi-PIFA antenna is designed to operate at LTE band 7 (2.6 GHz). The quasi-lumped patch which includes two parasitic capacitors, an inductor, and a network of interdigital capacitor is short-circuited to the ground at the end. The antenna operating frequency can be tuned not only by patch size, but also by the number of fingers (N), length (L_I), and width (W_C) of inductor and interdigital capacitors, respectively. The proposed antenna is fabricated in a 2D single layer while the conventional PIFA antennas usually are fabricated in 3D. This makes the fabrication process much easer and more precise. In addition, many components must be integrated above the ground plane and below the main resonator in conventional 3D PIFA which affect the antenna performance. The proposed antenna in this paper occupies much smaller volume compared to other kinds of PIFA antenna and is better choice for integration in small applications where the space is quite valuable. Also the strong dependency of PIFA on very sensitive parameter of conventional 3D-PIFA, its height, is eliminated using this approach. Although LTE band 7 is chosen as a sample frequency to show the antenna performance, it can be tuned to other desired frequencies by small variation in the affecting parameters which were discussed in this paper. The antenna has been examined in the laboratory which shows good agreement regarding simulation and measurement results.

Conflict of Interests

The authors declare that there is no conflict of interests regarding the publication of this paper.

Acknowledgment

The authors wish to thank Universiti Sains Malaysia for funding this project under USM Fellowship scheme and grant numbers 1001/PELECT/814202 USM RUT.

References

[1] D. A. Sanchez-Hernandez, *Multiband Integrated Antennas for 4G Terminals*, Artech House, 2008.

[2] M. R. Aghda, M. R. Kamarudin, and H. U. Iddi, "M-shape surrounded with ring patch wideband monopole printed antenna," *Microwave and Optical Technology Letters*, vol. 54, no. 2, pp. 482–486, 2012.

[3] M. Rafiee, M. F. Ain, and M. S. Aftanasar, "A novel UWB octagonal semi-ring antenna with CPW-wing-shaped ground plane," *Progress In Electromagnetics Research Letters*, vol. 41, pp. 113–123, 2013.

[4] H. T. Chattha, M. K. Ishfaq, Y. Saleem, Y. Huang, and S. J. Boyes, "Band-notched ultrawide band planar inverted-F antenna," *International Journal of Antennas and Propagation*, vol. 2012, Article ID 513829, 6 pages, 2012.

[5] M. Koubeissi, M. Mouhamadou, C. Decroze, D. Carsenat, and T. Monédière, "Triband compact antenna for multistandard terminals and user's hand effect," *International Journal of Antennas and Propagation*, vol. 2009, Article ID 491262, 7 pages, 2009.

[6] K. R. Boyle and P. J. Massey, "Nine-band antenna system for mobile phones," *Electronics Letters*, vol. 42, no. 5, pp. 265–266, 2006.

[7] P. Panaïa, C. Luxey, G. Jacquemod, R. Staraj, L. Petit, and L. Dussopt, "Multistandard reconfigurable PIFA antenna," *Microwave and Optical Technology Letters*, vol. 48, no. 10, pp. 1975–1977, 2006.

[8] L. Mo and C. Qin, "Tunable compact UHF RFID metal tag based on cpw open stub feed PIFA antenna," *International Journal of Antennas and Propagation*, vol. 2012, Article ID 167658, 8 pages, 2012.

[9] E. Bonek, P. Nowak, and J. Fuhl, "Improved internal antenna for hand-held terminals," *Electronics Letters*, vol. 30, no. 22, pp. 1816–1818, 1994.

[10] A. C. K. Mak, R. R. Rowell, R. D. Murch, and C.-L. Mak, "Reconfigurable multiband antenna designs for wireless communication devices," *IEEE Transactions on Antennas and Propagation*, vol. 55, no. 7, pp. 1919–1928, 2007.

[11] C.-H. Chang and K.-L. Wong, "Printed $\lambda/8$-PIFA for penta-band WWAN operation in the mobile phone," *IEEE Transactions on Antennas and Propagation*, vol. 57, no. 5, pp. 1373–1381, 2009.

[12] G. K. H. Lui and R. D. Murch, "Compact dual-frequency PIFA designs using LC resonators," *IEEE Transactions on Antennas and Propagation*, vol. 49, no. 7, pp. 1016–1019, 2001.

[13] J.-X. Liu and W.-Y. Yin, "A compact interdigital capacitor-inserted multiband antenna for wireless communication applications," *IEEE Antennas and Wireless Propagation Letters*, vol. 9, pp. 922–925, 2010.

[14] K. R. Boyle and L. P. Ligthart, "Radiating and balanced mode analysis of PIFA antennas," *IEEE Transactions on Antennas and Propagation*, vol. 54, no. 1, pp. 231–237, 2006.

[15] B. C. Wadell, *Transmission Line Design Handbook*, Artech House, Norwood, Mass, USA, 1991.

[16] G. D. Alley, "Interdigital capacitors a nd their application to lumped-element microwave integrated circuits," *IEEE Transactions on Microwave Theory and Techniques*, vol. 18, 1970.

[17] I. J. Bahl, *Lumped Elements for RF and Microwave Circuits*, Artech House, 2003.

[18] J.-S. G. Hong and M. J. Lancaster, *Microstrip Filters for RF/Microwave Applications*, John Wiley & Sons, 2004.

[19] M. Naghed and I. Wolff, "Equivalent capacitances of coplanar waveguide discontinuities and interdigitated capacitors using a three-dimensional finite difference method," *IEEE Transactions on Microwave Theory and Techniques*, vol. 38, no. 12, pp. 1808–1815, 1990.